

Cog-EEG: Early Detection of Cerebrovascular Patients With Cognitive Impairment Using EEG

Xiaomin Guo^{ID}, Luting Shen, Lan Li, Shan Chang^{ID}, Member, IEEE, Zongwei Liu,
and Yang Shi^{IF}, Member, IEEE

Abstract—The cognitive impairment caused by cerebrovascular disease is one of the most common causes of dementia in the elders. Cerebrovascular diseases are traditionally diagnosed by neuroimaging techniques, e.g., magnetic resonance imaging, which are however high-priced and can only identify the structural change of cerebral vessels. Questionnaire form-based diagnosis, e.g., mini-mental state examination (MMSE) or cognitive assessment (MoCA), is commonly used to discover cognition impairment, however subjective, highly relying on the experience of doctors. Electroencephalogram (EEG) waveform changes with physiological conditions and it is closely related to cognitive, so it is promising to identify cerebrovascular disease. In this work, we propose an EEG-based diagnosis approach, Cog-EEG, to distinguish between healthy people, cerebrovascular patients with and without cognitive impairment, effectively, which contains the following key designs. First, after preprocessing of EEG signals (i.e., electrode positioning, re-reference, filtering, segmentation, and independent component analysis), Cog-EEG exploits weighted minimum norm estimation to enable source localization with low-density (i.e., 19 channels) EEG signals, and then the recovered source signals are analyzed in time-frequency domain. Second, Cog-EEG conducts cross wavelet transform between brain regions, and extracts the corresponding functional connectivity matrices between them. Third, the functional connectivity matrices are utilized as key features and fed into a classifier for prediction. We collect an EEG signals dataset of 78 subjects, among whom 19 are healthy, 30 are cerebrovascular patients with cognitive impairment, and the rest are cerebrovascular patients without cognitive impairment. Experimental results demonstrate that Cog-EEG can achieve a classification accuracy of 96.7%.

Index Terms—Cerebrovascular, cognitive impairment, cross wavelet transform (XWT), functional connectivity matrix, low-density electroencephalogram (EEG) signal.

Received 22 October 2024; revised 4 December 2024; accepted 17 December 2024. Date of publication 10 January 2025; date of current version 9 May 2025. This work was supported in part by the Shaanxi Provincial Key Research and Development Program Project under Grant 2023-ZDLSF-20; in part by the Natural Science Foundation of Shanghai under Grant 22ZR1400200; and in part by the Fundamental Research Funds for the Central Universities under Grant 2232023Y-01. (Corresponding author: Shan Chang.)

This work involved human subjects or animals in its research. Approval of all ethical and experimental procedures and protocols was granted by the Shaanxi Provincial People's Hospital Ethics Committee.

Xiaomin Guo is with the School of Department of Neurology, Shaanxi Provincial People's Hospital, The Third Affiliated Hospital of Xi'an Jiaotong University, Xi'an 710000, China (e-mail: guoxiaomin@xjtu.edu.cn).

Luting Shen, Lan Li, and Shan Chang are with the School of Computer Science and Technology, Donghua University, Shanghai 201620, China (e-mail: changshan@dhu.edu.cn).

Zongwei Liu is with the First Institute of Oceanography, Ministry of Natural Resources, Qingdao 266061, China (e-mail: liuzongwei@fio.org.cn).

Yang Shi is with the School of Marine Science and Technology, Northwestern Polytechnical University, Xi'an 710072, China (e-mail: shiyang@nwpu.edu.cn).

Digital Object Identifier 10.1109/JIOT.2025.3525654

I. INTRODUCTION

IN RECENT years, the proportion of dementia caused by cerebrovascular disease has been increasing with the development of population aging in the world. Early detection of cerebrovascular patients with cognitive impairment is crucial for timely intervention and treatment of dementia, however very challenging. Traditional imaging examinations, such as magnetic resonance imaging (MRI) or computed tomography (CT), can discover structural damages of blood vessel. However, dementia patients can only be detected in severe or late stages through imaging, and cannot be identified in the early stages. The common practice for identifying mild cognitive impairment (MCI) requires answering standard questionnaires by the patients and detailed consultations with experienced doctors, which implies the diagnostic results are of high subjectivity and randomness. Most advanced techniques available to diagnose dementia and differentiate cognitive impairment are based on molecular imaging, however, the use of which is limited due to high cost.

There are tens of thousands of neurons in the human brain, and the electrical signals generated by the activities between these neurons are called brainwaves, and are closely related to the functional status of brain. Brainwaves of dementia patients may have distinguishing features compared to those normal people, e.g., focal slow waves, diffuse slow waves, or both [1]. Electroencephalogram (EEG) is an inexpensive and effective way of recording brainwaves, which has been used for the diagnosis or prediagnosis of various disorders, including dementia, paralysis, Parkinson's disease, Schizophrenia, and so on [2]. Ieracitano et al. analyzed the power spectral density of 19 channels EEG signals and represented the corresponding spectral distributions as a 2-D grayscale image. Then, a convolutional neural network was utilized for classification of Alzheimer's disease (AD), MCI, and healthy controls (HCs), obtaining an average prediction accuracy of 83.3%. Ding et al. collected resting state EEG signals of HC, amnestic MCI and AD patients, and extracted the spectral power, complexity of the EEG signal from each brain region, as well as analyzed the functional connectivity between brain regions. Experimental results indicate that, with the progress of the AD, the brain activities slow down, EEG signal complexity decreases, and connectivity between brain regions weakens. However, they failed to analyze the correlations between EEG signals of different brain regions, which may demonstrate distinguishing features for those dementia patients. For example, their synchronization might diminish or even completely disappear.

The existing work typically utilizes one or several statistics of cross features extracted from a pair of EEG signals as the indicator of connectivity between two relevant brain regions, for example, the spectral coherence, phase locking value (PLV), spectral entropy, mutual information (MI) [4], etc., which however demonstrates poor performance when being used to detect MCI. The reason is that those coarse-grained cross features can not capture the small connectivity changes of MCI patients. The most relevant work was proposed by Adebisi et al. [5], which characterizes stages of brain functional networks of MCI, Alzheimer and vascular dementia patients in comparison with healthy people by MI, only achieving an accuracy of 82.1%. Furthermore, most of the related work requires high-density EEG signals with 64–256 electrode channels from high-end EEG acquisition equipment, which supports accurate source localization of EEG signals, but is expensive and not widely available.

In this article, considering that portable and low-density EEG equipment is relatively commonly used, it is desired to use low-density EEG signals to identify cerebrovascular patients with and without cognitive impairment, and normal individuals, which however confronts with two challenges. First, source localization requires high-density EEG, but the EEG data we collected is low-density. So, it is challenging to enable source localization with low-density EEG. Second, it is challenging to find a fine-grained representation that can effectively reflect the correlation of activities between different brain regions. To solve the above challenges, we propose, Cog-EEG, a time–frequency analysis method, the efficacy of which is demonstrated by an EEG dataset of 78 participants, collected by the digital EEG detector SOLAR2848B. First, we preprocess the EEG data, including electrode positioning, re-reference, filtering, segmentation, and independent component analysis (ICA). Second, we introduce minimum norm imaging to enable accurate low-density EEG signal source localization, converting the 19 channels EEG data into 16 brain regions, and then the recovered source signals are analyzed in time–frequency domain. Third, the time–frequency correlation of EEG signals between different brain regions is calculated by cross wavelet transform (XWT), and then the wavelet cross-spectrum (i.e., a complex matrix) is extracted from the cross-spectrum obtained, and used as functional connection features. Then, those features are used to train the classifier. Finally, we conduct comprehensive experiments on the EEG dataset, including different events, features, classifiers, and methods of functional connectivity, and also conduct source localization ablation experiment which demonstrates that source localization can improve classification performance. Experimental results demonstrate that the classification accuracy of our method is over 96.0%.

We summarize the contributions of this work as follows.

- 1) An EEG signal dataset is constructed, and it contains 59 patients with cerebral small vessel disease (CSVD) who were admitted to the People's Hospital of Shaanxi Province from September 2022 to September 2023. They were divided into the group with cognitive impairment (cerebral small vascular with cognitive impairment, CSVC+D group, $n = 30$) and the group

without cognitive impairment (CSVD group, $n = 29$), while 19 HCs were recruited as the control group (HC group). EEG was performed in the three groups.

- 2) We propose to use XWT to calculate the time–frequency correlation of different brain regions, and extract a fine-grained feature matrix to represent the relation between brain regions.
- 3) Experiments are conducted to evaluate the effectiveness of our method.

This article is organized as follows. Section II discusses related works. Section III introduces how to collect the data and the information of data. Section IV elaborates on the designs of the proposed methods. Section V gives the implementation of the proposed method and presents performance evaluation results, and Section VI concludes this article.

II. RELATED WORK

As a key technology to detect changes in electrical signals in brain nerve tissues, EEG has attracted extensive attention due to its unique advantages of high temporal resolution, safety, and convenience.

A. Time–Frequency Analysis of EEG

There are two main ways for time–frequency analysis, the first one is to estimate power of signal at each specific time–frequency point, and the main techniques include short-time Fourier transform and wavelet transform. Murugappan et al. [7] used discrete wavelet transform to calculate the proportion of sub-band energy, the energy of the sub-band, and the root mean square of the wavelet coefficient of the α band, and realized classification of emotion. Adebisi et al. [5] calculated MI based on the time–frequency maps of brain waves from different channels, so as to classify healthy people, vascular dementia, AD and MCI. The second one is to decompose signal into a set of superimposed components with specific time–frequency characteristics, and explore different waveform meanings of the brain through event-related potentials which refer to EEG segments with constant waveform and latency formed after superimposed averaging. Arias-Cabarcos et al. [8] trained a model based on P300 and N400 event potential obtained from auditory stimuli, and used brainwaves as a bio-metric feature to achieve user authentication.

B. Image-Based Detection of Cognitive Impairment

Cognitive impairment can be diagnosed by neuroimaging techniques, such as CT, MRI, positron emission tomography (PET), and so on, which can examine patients in terms of structure and function. Ieracitano et al. [9] analyzed the power spectral density of 19-channel EEG signals, expressed the associated spectral distribution as a 2-D grayscale image, and then achieved an average accuracy of 83.3% in a three-categorical experiment with 189 subjects (63 each of AD, MCI, and HC) using a convolutional neural network. Rabeh et al. [10] extracted three regions of interest, namely, the hippocampus, corpus callosum, and cortex, and independently classified the subjects based on each region, then merged the

results by using a decision tree. The subjects are ultimately classified into three categories: 1) AD; 2) MCI; and 3) healthy individuals. Chen et al. [11] proposed resting state functional MRI samples based on different AD patients and analyzed four different subtypes of AD based on connectivity biomarkers, the differences in functional connectivity, brain structure, and cognitive abilities between these subtypes. The electromagnetic radiation generated by these detection methods may cause damage to patients, and the hardware equipment is complex, and the cost is relatively high.

C. EEG-Based Detection of Cognitive Impairment

Clinically, the recorded brain electrical activity will be used to analyze, interpret related diseases to assist diagnosis. EEG is the overall reflection of electrophysiological activity of brain nerve cells in the cerebral cortex. EEG is widely used because of its noninvasiveness, safety, low price, and reliability. Due to damage of intracranial neurons and brain tissues in patients with cognitive impairment, the physiological electrical signals generated by the superposition of neuronal cell populations will change. Because it is sensitive and objective, EEG can be effectively used to characterize cognitive function. Ding et al. [12] extracted spectral power, complexity and functional connectivity from resting-state EEG data of 113 healthy subjects, 116 patients with amnesic MCI, and 72 AD patients, and evaluated classification performance from multiple perspectives. The results show that with the progression of AD, brain activity tended to slow down, complexity decreased and connectivity weakened. Bayot et al. [13] analyzed correlation between gait freezing and brainwave functional connectivity by comparing spectral power maps and frontoparietal functional connectivity networks of different frequency bands of EEG in Parkinson's disease patients with and without gait freezing and healthy individuals.

III. DATA COLLECTION

We collect an EEG dataset which contains 78 participants (31 women and 47 men) using the digital EEG detector (SOLAR2848B) from Beijing Sun Company. The process of data collection is shown in Fig. 1. In the dataset, there are 19 healthy subjects, 59 cerebrovascular patients (where 29 cases of CSVD patients and 30 cases of CSVD+D patients) who were hospitalized in Shaanxi Provincial People's Hospital from September 2022 to September 2023. Among them, 19 cases of health control were collected as the control group within the same period. The inclusion criteria were as follows: 1) age of 50–85 years old; 2) examination in accordance with the diagnostic criteria of China's 2021 edition of the Chinese Consensus on the Diagnosis and Treatment of CSVD (13); and 3) complete clinical data of patients or family members who are willing to join this study. The exclusion criteria were as follows: 1) large cerebral infarction, cerebral hemorrhage, and other macrovascular lesions; 2) encephalitis, normal pressure hydrocephalus, Alzheimer's, Parkinson's, and other neurological diseases that cause cognitive dysfunction; 3) other systemic diseases that cause cognitive changes, such as diabetes mellitus, obesity, and metabolic disorders; 4) people

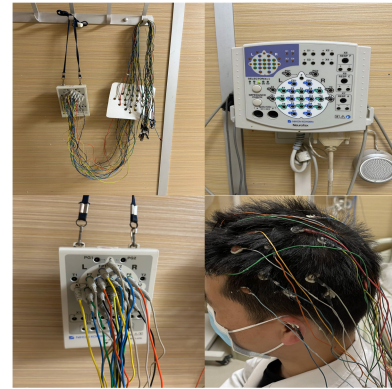


Fig. 1. Process of data collection.

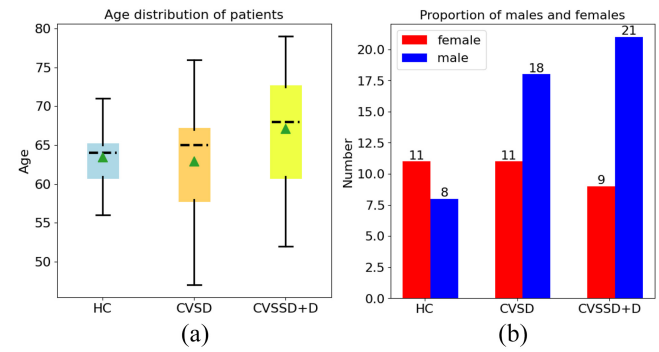


Fig. 2. (a) Age distribution of patients in our EEG dataset. (b) Proportion of males and females in our EEG dataset.

with color blindness and color weakness; 5) people with severe hearing, reading, and writing disorders; and 6) subjects with contraindications to MRI, such as metal implants and claustrophobia. All subjects will be informed and sign a written informed consent form.

The brainwave (15 mins) of each person is recorded during eyes opening (EO, 3 times, each for 2 mins), eyes closing (EC, 3 times, each for 2 mins), and hyperventilation (HV, 3 mins), respectively. The true labels come from relevant questionnaire and diagnosis of professional doctor. The names, ages of each subject are recorded. The youngest is 47 and the oldest is 83. The age distributions of different types of participants are shown in Fig. 2(a). The sex composition is shown in Fig. 2(b). HC is healthy subject, CVSD is cerebrovascular patient without cognitive impairment, CVSD+D is cerebrovascular patient with cognitive impairment.

The study involving humans was approved by Shaanxi Provincial People's Hospital Ethics Committee. The study was conducted in accordance with the local legislation and institutional requirements. The participants provided their written informed consent to participate in this study. The participants' privacy information is protected, e.g., we use pseudo names instead of real names.

IV. COG-EEG DESIGN

The pipeline (shown in Fig. 3) of our approach includes preprocessing of EEG data, source localization, constructing correlation graph between brain regions, and feature

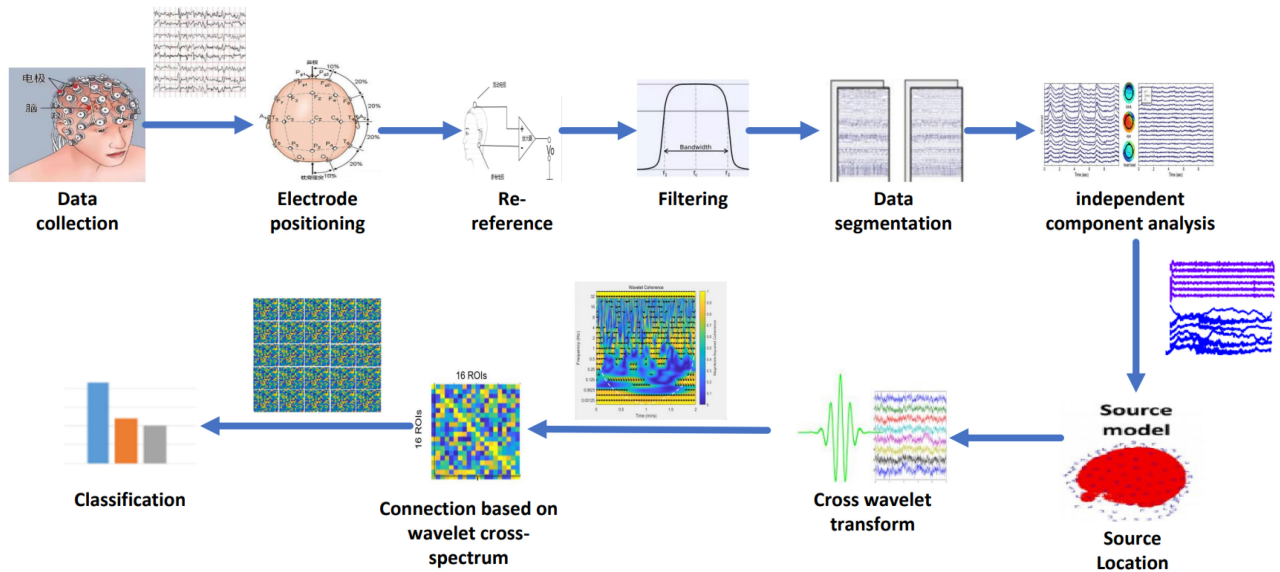


Fig. 3. Overview of Cog-EEG.

Algorithm 1 Cog-EEG

Input: the EEG signals $X(t)$, the time sampling points T , the number of EEG channels M , the EEG channels $\{C_1, C_2, \dots, C_M\}$, the classifier CLF

Output: the result of classifier y

- 1: $X(t) \leftarrow (x_{FP1}(t), x_{FP2}(t), \dots, x_{A2}(t))^T$
- 2: Using A1 and A2 as reference electrode to re-reference:
- 3: $x_n(t) \leftarrow x_n(t) - \frac{1}{2}(x_{A1}(t) + x_{A2}(t))$
- 4: $X(t) \leftarrow X(t), 0 \leq t \leq T$ no greater than 50Hz
- 5: $X(t) \leftarrow dataSegment(X(t))$
- 6: $X(t) \leftarrow ICA(X(t))$
- 7: $\widehat{S} \leftarrow sourceLocalization(X(t))$
- 8: $FC \leftarrow functionalConnection(\widehat{S})$
- 9: $y \leftarrow CLF(FC)$
- 10: **return** y

extraction (i.e., construction of functional connectivity matrix based on wavelet cross spectrum), as well as classification. Preprocessing includes electrode positioning, re-reference, filtering, segmentation, and ICA. Source localization converts EEG data recorded by electrodes into different brain regions. We calculate XWT between different brain regions, and utilize wavelet cross spectral features to construct functional connectivity between brain regions. These features are further fed into a classifier for prediction. The algorithm of the overall process of the Cog-EEG is shown in Algorithm 1.

A. EEG Preprocessing

1) Electrode Positioning: Electrode positioning is to match different signals to corresponding channels according to the adopted electrode placement standard. Using the international 10–20 standard electrodes system, a total of 19 scalp electrodes and 2 ear electrodes were placed. The scalp electrodes are named as FP1, FP2, F7, F3, FZ, F4, F8, T7, C3, CZ, C4, T8, P7, P3, PZ, P4, P8, O1, and O2 according to the brain

TABLE I
INTERNATIONAL 10–20 STANDARD ELECTRODE PLACEMENT

region	electrode	region	electrode
Frontal Pole	FP1 FP2	Inferior Frontal	F7 F8
Frontal	F3 FZ F4	Central	C3 CZ C4
Parietal	P3 PZ P4	Occipital	O1 O2
Temporal	T3 T4	Posterior Temporal	T5 T6
Auricular	A1 A2		

regions, and the two ear electrodes are A1 and A2, as shown in Table I. So there are total of 21 corresponding EEG channels. Each EEG channel is represented by a vector $x_n(t)$, where n is the scalp electrode, t is time. M is the number of EEG channels (i.e., $M = 21$). T is the transpose operation. So, an EEG sample at time t is represented by $X(t) \in R^M$

$$X(t) = (x_{FP1}(t), x_{FP2}(t), \dots, x_{A2}(t))^T. \quad (1)$$

2) Re-Reference: Re-reference selects the 0 electrode as the reference electrode [15]. We adopt bipolar reference, which uses two less active electrodes in the left and right brain as the reference electrode, to weaken the effect of interference. We use A1 and A2 as reference electrode, and take the average value of two mastoid data as the reference data, which is called bilateral mastoid reference

$$x_n(t) = x_n(t) - \frac{1}{2}(x_{A1}(t) + x_{A2}(t)). \quad (2)$$

3) Filtering and Data Segmentation: A band-pass filter is applied to attenuate components beyond EEG signals from 0 to 50 Hz, called 0–50-Hz low-pass filter. The primary function of filtering in this is noise reduction. Each channel of each participant slides a window of fixed length z in time. Because the frequency range of EEG signals is mainly from 0 to 50 Hz, we ignore the frequency of EEG signals higher than 50 Hz to prevent interference from high-frequency signals, such as electromyography or other noise signals, and to ensure that the fast wave of EEG signals are not interfered.

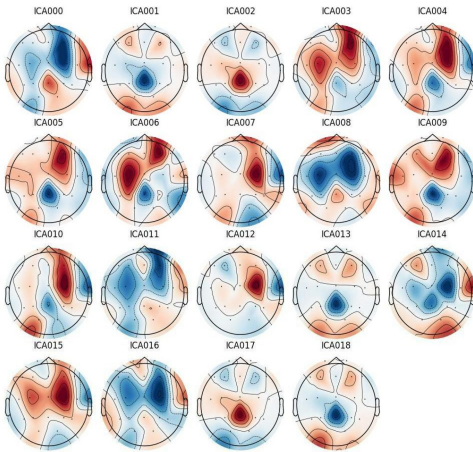


Fig. 4. Results of ICA.

The recorded EEG data is composed by three different types of events (i.e., EC, EO, and HV). So according to types of events, the starting and end points, the EEG data can be split into different segments. It can be broken down into smaller segments if needed, such as 1 min.

4) Independent Component Analysis: EEG signals are susceptible to noise components, such as eye movement and power frequency interference. ICA assumes that the signal source is an instantaneous linear mixture of brain signals and artifact signals, and that each source signal is statistically independent, and that the dimension of observation is greater than or equal to the dimension of the source signal, and that at most one of each source signal is Gaussian, then the observed signal can be decomposed into independent components. That is, assuming that the collected EEG signal is a linear mixture of various EEG components and artifact components, and the number of source components is less than the number of channels, and the mixed signal is separated to obtain different components, and then further judged to remove the signal components that do not belong to EEG, such as eye movement and heartbeat. In brief, this approach first breaks up an EEG into multiple modes or signature signals, then applies mix source separation (MSS) to extract EMG-free source components and reconstruct the clean EEG [16].

The abscissa of original EEG data is time point, and the ordinate is different channels, which need to be unmixed through the ICA matrix. The ICA matrix is a matrix between channel and component, and each value is equivalent to the proportion of signal of each channel corresponding to each component, and the other seven components are generally found [17]. The IC topographic map is actually the inverse matrix of the ICA matrix. Through ICA, a topographic map of 19 components can be obtained [18], as shown in Fig. 4.

B. Source Localization

The tissues in the brain, including scalp, skull, cerebrospinal fluid, etc., have strong or weak electrical conduction properties. Because of the conduction effect, source activity in the brain is transmitted not only directly above the scalp,

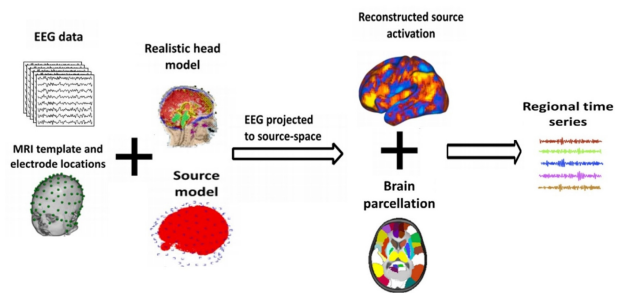


Fig. 5. Source localization.

but also to other locations in the scalp. The collected EEG signals reflect the conduction results of electrical activity in the cerebral cortex. If the collected signals are directly analyzed, it is very limited in revealing the interactive activities within the brain. Source localization is to infer the source distribution of EEG activity from recorded EEG data, and source distribution of EEG activity includes information of source direction, localization and intensity. Source localization can reduce volume conduction effects. EEG structure requires EEG signals, electrode 3-D coordinates on scalp, head model, and source model, as shown in Fig. 5. The head model is usually calculated by boundary element method (BEM) combined with the MRI image of subject [19]. BEM is a numerical technique for calculating the surface potential generated by current sources in segmented uniform volume conductors. Combining EEG data, MRI template, electrode position, estimation of head model, and calculation of source model, we can project EEG signal recorded by electrode into source space and obtain reconstructed source activity. According to the regional layout of brain, EEG time-series signal on each region is calculated. Here, the minimum norm imaging method suitable for low-density EEG data is used for source localization. By constructing a weighted minimum norm estimation (wMNE) source model, the current source density and spectral power are estimated based on the frequency bands of each vertex in the source model, and the EEG amplitude is determined [20]. Based on the brain regional layout of the vcAltas, EEG signals are inverted onto 16 source domains [16], and then time-frequency correlations of EEG signals in different brain regions are studied.

The dynamics of cortical sources from scalp EEG data [i.e., determining the position, orientation, and magnitude of dipolar sources $\hat{S}(t)$] is reconstructed. Since the cortical sources have fixed position and orientation (centroids of Desikan–Killiany regions, normal to the cortical surface), the inverse problem is reduced to compute the magnitude of dipolar sources $\hat{S}(t)$

$$\hat{S}(t) = W \cdot X(t) \quad (3)$$

where W is based on different assumptions related to the spatiotemporal properties of the sources and regularization constraints

$$W = BG^T(GBG^T + \lambda C)^{-1} \quad (4)$$

Algorithm 2 Source Localization

Input: the EEG signals $X(t)$, the gain (leadfield) matrix G , the noise covariance matrix C , the regularization parameter λ , the time sampling points T

Output: the dipolar source signal \widehat{S}

- 1: Calculate the source signal of each time sampling points $\widehat{S}(t)$.
- 2: **for** t in T **do**
- 3: Calculate the diagonal matrix B from G :
- 4: $B_{ij} \leftarrow \begin{cases} (G_i^T G_i)^{\frac{1}{2}} & \text{if } i = j \\ 0 & \text{if } i \neq j \end{cases}$
- 5: $W \leftarrow BG^T(GBG^T + \lambda C)^{-1}$
- 6: $\widehat{S}(t) \leftarrow W \cdot X(t)$
- 7: **end for**
- 8: Construct \widehat{S} using the source signal in each time sampling points:
- 9: $\widehat{S} \leftarrow \{\widehat{S}(t_1), \dots, \widehat{S}(t_n)\} // \{t_1, \dots, t_n\} = T$, n is the number of T
- 10: **return** \widehat{S}

where G is the $(M \times P)$ Gain (*leadfield*) matrix, λ is the regularization parameter, and computed based on the signal-to-noise ratio (SNR): $\lambda = 1/\text{SNR}$, and the SNR depends on the data type. C is the noise covariance matrix (set as the identity matrix in our case). G describes the contribution of each cortical source to scalp signals by taking into account the geometrical and electrical characteristics of the head. The matrix B is a diagonal matrix built from matrix G with nonzero terms inversely proportional to the norm of lead field vectors. This matrix adjusts the properties of the solution by reducing the bias inherent to the standard MNE solution

$$B_{ij} = \begin{cases} (G_i^T G_i)^{\frac{1}{2}}, & \text{if } i = j \\ 0, & \text{if } i \neq j. \end{cases} \quad (5)$$

The details of getting the dipolar source signal \widehat{S} are shown in Algorithm 2.

C. Constructing Correlation Graph Between Brain Regions

XWT is constructed from continuous wavelet transform (CWT) of two time series to reveal common power and relative phase in time–frequency space [22]. The CWT can jointly analyze the time and frequency of the signal, which can better locate the transient in the signal and detect the time and local oscillation of the nonstationary signal. The crossed wavelet transform compares the power and phase relationships and compares the time-varying correlation between two signals on the basis of the time–frequency diagram obtained by the CWT [23]. XWT can measure the time–frequency correlation between two signals in a more fine-grained dimension, and locate delay or stagnation of signal interaction activity in different brain regions of patients with cognitive impairment. The calculation is done by multiplying the continuous wavelet matrix of the time series X by the continuous wavelet complex conjugate matrix of the time series Y . The formula is shown in

$$C_{xy}(a, b) = S(C_x^*(a, b)C_y(a, b)) \quad (6)$$

where a and b denote scales and positions, respectively, S is a smoothing operator on time and scale, the superscript * represents complex, $C_x^*(a, b)$ and $C_y(a, b)$ are the CWT at scale a and position b , and $C_{xy}(a, b)$ is the crossed wavelet transform sought.

We calculate XWT of the full frequency range of EEG signals from two different brain regions. The output of XWT includes wavelet coherence matrix (wcoh), wavelet cross spectrum complex matrix (wcs), cone of influence, and CWT matrix. Wavelet coherence can indicate consistency between two signals. In wavelet spectrum, the phase relation is represented by arrows. The phase hysteresis relation of two signals is represented by a specific direction. The right arrow represents a phase of positive correlation, the left arrow represents a phase of the opposite, the down arrow represents a phase of X ahead of Y , and the up arrow represents a phase of X behind Y .

According to EEG waveform of different patients, the signal time series of two different brain regions are selected to calculate XWT, and cross wavelet spectra between 16 brain regions are obtained. The cross wavelet spectra of the participant D022 (healthy people), D074 (cerebrovascular patient without cognitive impairment), and D053 (cerebrovascular patient with cognitive impairment) are shown in Fig. 6. It can be observed that time–frequency correlation between hOc1 (human Occipital cortex 1) Left and hOc1 Right brain regions gradually weakened with the deepening of cognitive impairment [21], which suggests that cognitive impairment may affect consistency of EEG signals between different brain regions.

D. Extracting Functional Connectivity Matrix From XWT

To calculate functional connectivity on source domain, it is necessary to select appropriate methods. The wavelet cross spectral features obtained from XWT are complex matrices, with values composed of real and imaginary parts. We use two methods to calculate functional connectivity. The first method called average dividing is to divide this matrix into $f \times e$ time–frequency areas (f equal frequency bands; e equal time periods), calculate the average of the imaginary parts of the wavelet cross spectral within each grid, remove the mean of the last row grid where the influence cone is located, and obtain a wavelet cross spectral matrix of $(f-1) \times e$ between these two brain regions, and use this to establish functional connections between different brain regions. The other one called 5-band dividing is to divide this matrix into $5 \times e$ time–frequency areas (five bands: delta (0.5–4 Hz), theta (4–8 Hz), alpha (8–12 Hz), beta (12–30 Hz), and gamma (30–50 Hz); e equal time periods) [22], calculate the average of the imaginary parts of the wavelet cross spectral within each grid, and obtain a wavelet cross spectral matrix of $5 \times e$ between these two brain regions, and use this to establish functional connections between different brain regions. Using XWT to measure the correlation of EEG signals in different brain regions, the time–frequency correlation maps of the two signals obtained from wavelet transform are averaged, combined together, and transformed into a functional connectivity matrix [24], as shown

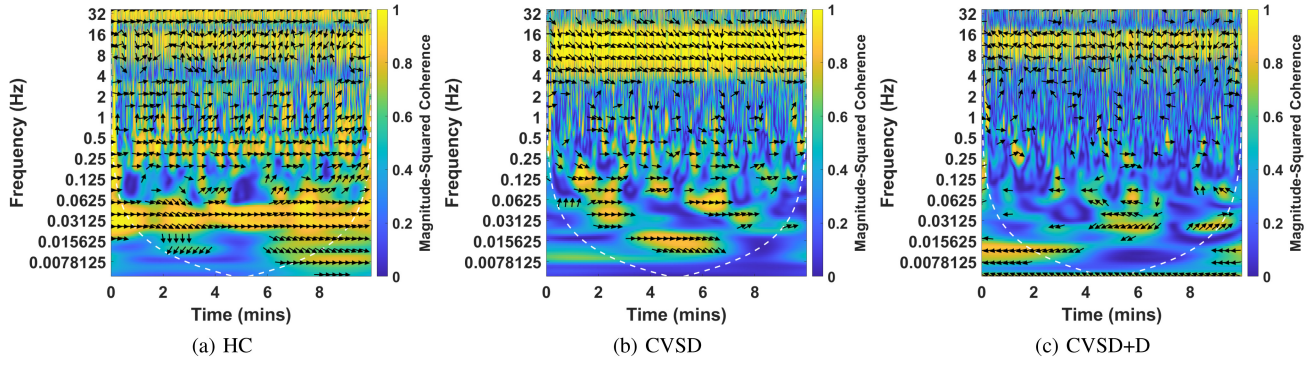


Fig. 6. XWT of hOc1 L-hOc1 R. (a) HC. (b) CVSD. (c) CVSD+D.

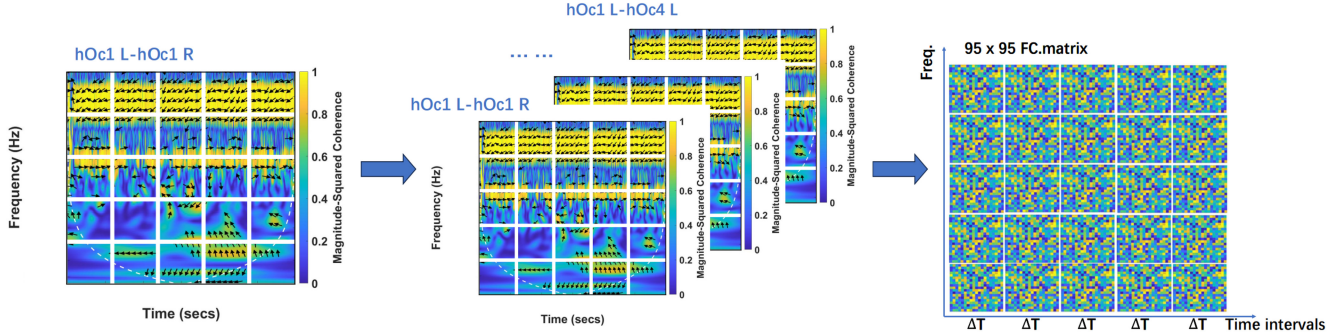


Fig. 7. Functional connection based on wavelet-cross spectrum.

Algorithm 3 Functional Connection

Input: the number of EEG channels M , the EEG channels $\{C_1, C_2, \dots, C_M\}$, the EEG signal or the dipolar source signal $X = \{x_{C_1}, x_{C_2}, \dots, x_{C_M}\}$

Output: the functional connectivity matrix FC

- 1: Initialize $cnt \leftarrow 0$
- 2: **for** i in $\{C_1, C_2, \dots, C_{M-1}\}$ **do**
- 3: **for** j in $\{C_{i+1}, \dots, C_M\}$ **do**
- 4: Calculate the wavelet cross spectrum complex matrix wcs :
- 5: $wcs_{cnt} \leftarrow XWT(x_i, x_j)$
- 6: Only take the imaginary part of wcs:
- 7: $wcs_{cnt} \leftarrow Im(wcs_{cnt})$
- 8: $wcs_{cnt} \leftarrow mean(wcs_{cnt})$
- 9: $cnt \leftarrow cnt + 1$
- 10: **end for**
- 11: **end for**
- 12: $FC \leftarrow splice(wcs_0, \dots, wcs_{cnt})$
- 13: **return** FC

in Fig. 7. The functional connectivity matrix composed of different brain regions can reflect the signal interaction activity of all brain regions and can be used as EEG features for further classification. The algorithm of calculating functional connectivity is shown in Algorithm 3.

E. Classification

We use support vector machine (SVM) where we use C-support vector classification (SVC) and we set the kernel

function to radial basis function (rbf), the regularization parameter (C) to 10, and the kernel coefficient (gamma) to 0.1, to classify healthy individuals and cerebrovascular disease patients with and without cognitive impairment. There are a total of 1170 samples, one of which is a functional connectivity matrix constructed from wavelet cross spectral calculated from 1 min of EEG signals from two different brain regions of a subject. Test size is 20%. The optimal regularization constant and kernel variance are obtained using the grid search algorithm. Tenfold cross validation is performed with optimum parameters. Since SVM is a binary classifier, one versus all approach is used.

V. EVALUATION

A. Experimental Setup

We use the MATLAB plugin EEGLab for data preprocessing [25], and Python for source localization of EEG. Our code is based on Python's open-source MNE library for visual analysis of human neurophysiological data. The code is compiled on the TensorFlow platform to complete batch processing and three classifications of EEG signals.

Each EEG data is a total of 15 min (i.e., three alternating 2-min EO, 2-min EC, and one 3-min HV). Depending on three types of events, the starting and end points, the EO and EC data are three segments, 2 min each, the HV is one segment, for 3 min. It can be split into smaller segments if needed, such as 1 min. In our experiments, the EEG data is split into 15 segments, each segment for 1 min (i.e., the EO and EC data are both five 1-min segments, and the HV is three 1-min segments).

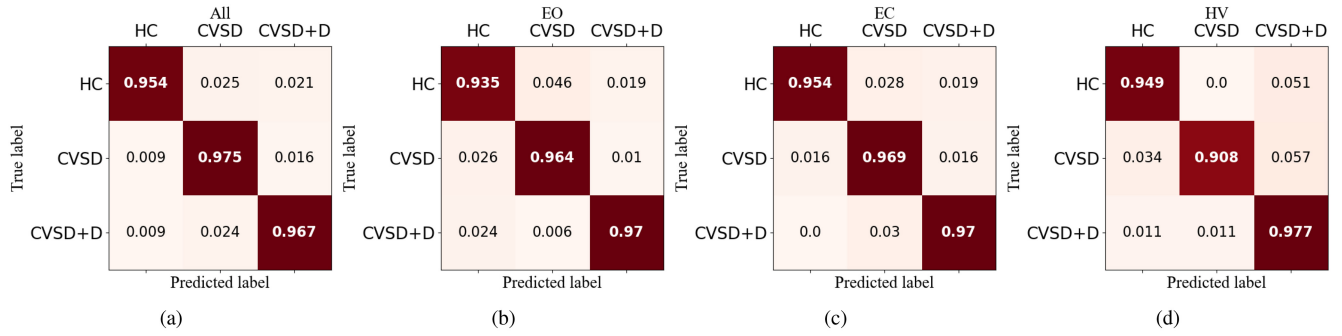


Fig. 8. Confusion matrix. (a) All events. (b) Under EO event. (c) Under EC event. (d) Under HV event.

TABLE II
OUTPUT RESULTS WITH HEALTHY PEOPLE AS POSITIVE EXAMPLES

Predicted		HC	CVSD	CVSD+D
Actual	HC	TP	FN	FN
CVSD	FP	TN	FN	FN
CVSD+D	FP	FN	TN	

B. Metrics and Comparison Method

1) *Metrics*: Table II enumerates all possible outputs, TP means an outcome where the model correctly predicts the positive class, TN means an outcome where the model correctly predicts the negative class, FP means an outcome where the model incorrectly predicts the positive class, and FN means an outcome where the model incorrectly predicts the negative class. We use accuracy, precision, recall, and F1 score as evaluation criteria for these three classification problems. Accuracy is the number of correctly classified samples in the total sample. Precision is the probability that a predicted positive sample is actually positive. Precision is calculated according to (7) and Table II. Recall is the percentage of positive samples correctly predicted. Recall is calculated according to (8) and Table II. The multiclass classification problem has no clear positive and negative samples, and is treated as a multiple binary problem. Healthy people, cerebrovascular patients with and without cognitive impairment take turns to act as positive samples. Macro means calculating precision and recall on the basis of many binary problems, then averaged, obtaining macro precision and macro recall. F1 score is calculated according to (9) based on precision and recall

$$\text{precision} = \frac{\text{TP}}{\text{TP} + \text{FP}} \quad (7)$$

$$\text{recall} = \frac{\text{TP}}{\text{TP} + \text{FN}} \quad (8)$$

$$\text{F1 score} = \frac{2 * \text{precision} * \text{recall}}{\text{precision} + \text{recall}} \quad (9)$$

2) *Comparison Method*: We compare the method proposed by Adebisi [7]. To identify the frequent subgraph related to dementia, the comparison method, first, formulates the brain functional network based on the phase information of EEG with MI as a measure. Then, the whole network is divided into subregions and frequent subgraph search is performed [5]. The primary difference is how to calculate the features. The

TABLE III
CLASSIFICATION PERFORMANCE

	Accuracy	Precision	Recall	F1 Score
XWT	96.7%	96.7%	96.5%	96.6%
A. T. Adebisi [5]	82.1%	82.2%	81.3%	81.7%

comparison method is to calculate MI according to the time-frequency maps of brainwave signals of different channels, set thresholds, extract key regions, and perform frequent subgraph mining to obtain functional connection features. In contrast, our method is that using XWT based on a finer granularity calculates the features.

C. Overall Performance

For a three-classification problem, there are many possible results. Fig. 8(a) shows confusion matrix of all EEG data. The cerebrovascular patients without cognitive impairment have the highest probability of being predicted successfully, and cerebrovascular patients without cognitive impairment are easily misclassified as those with cognitive impairment. Fig. 8(b)–(d) shows confusion matrix under EO event, EC event, and HV event, respectively. Table III shows accuracy, precision (macro), recall (macro), and F1 score achieved by ours method, which are better than reference method. Compared to the method in [5], our method computes features based on finer granularity. We visualize results with receiver-operating-characteristic (ROC) curves shown in Fig. 9(a). Compared with Adebisi et al. [5], XWT increases the area under the ROC curve (AUC).

D. Impact Factors

1) *Events*: The EEG waveform of different patients under EO, EC, and HV is recorded in dataset, and the classification performance of EEG under different events is counted. As shown in Table IV, the classification accuracy under EC is the closest to all EEG data, and the classification performance under HV and EO is relatively low. The results indicate that for EEG analysis of cognitive impairment, the resting state EEG is the most effective. Under eyes opened and HV, external interference may affect the attention status of the patients.

2) *Time-Frequency Features*: Table V compares effects of different eigenvalues on the classification performance of EEG data, including wavelet coherence, real and imaginary parts of

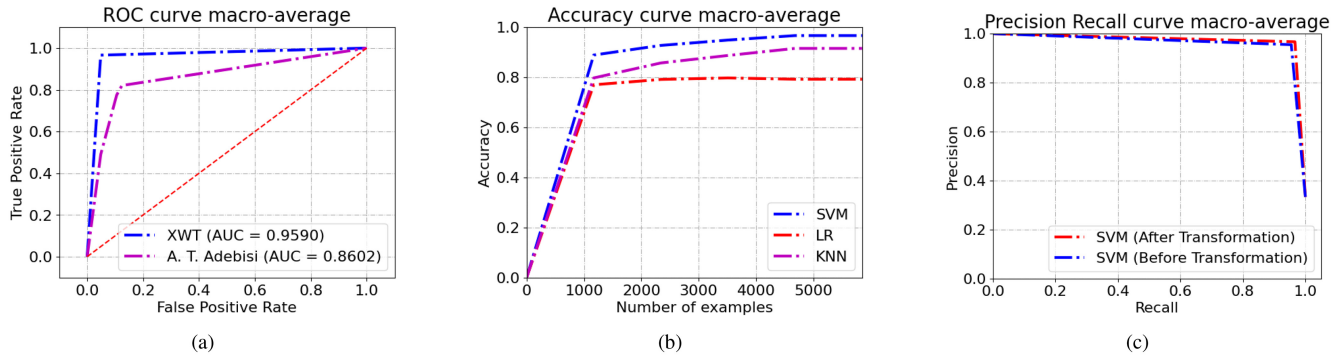


Fig. 9. (a) ROC curve. (b) Performances of different classifiers under different number of training samples. (c) PR curve with and without source localization.

TABLE IV
PERFORMANCE UNDER DIFFERENT EVENTS

	Accuracy	Precision	Recall	F1 Score
All	96.0%	96.1%	95.9%	96.0%
EO	96.6%	96.9%	96.2%	96.5%
EC	93.8%	93.3%	94.0%	93.6%
HV	94.9%	95.9%	94.5%	95.0%

TABLE V
CLASSIFICATION ACCURACY OF DIFFERENT FEATURES

	All	EO	EC	HV
Wavelet coherence	80.2%	75.6%	75.8%	67%
Wavelet cross spectrum.imag	96.7%	96.7%	96.5%	96.6%
Wavelet cross spectrum.real	82%	74.1%	74.3%	65.5%

wavelet cross spectrum [26]. Overall, under most of the events, the imaginary part has best classification performance. The results show that, in low-density EEG data, XWT can better reflect differences in power and phase of EEG than previous time-frequency correlation calculation methods.

3) *Classifiers*: Fig. 9(b) compares accuracy using different machine learning classifiers, including SVM, logistic regression (LR), and K -nearest neighbors (KNNs). After using grid search to find optimal parameters, the classification performance of SVM is optimal. With the increase of training sample size, the accuracy increases. When the number of training samples is 1000, SVM achieves 70% accuracy, and then this accuracy increases gradually. In the end, SVM achieves 96.7% accuracy, and LR and KNN also achieve nearly 80% accuracy.

4) *Division of Frequency*: Table VI compares accuracy using different methods of functional connectivity that are mentioned in Section IV-E. According to the first method, i.e., average dividing, we divide the matrix into 5×5 time-frequency areas, which only achieves 95.8% accuracy. And according to the second method, i.e., 5-band dividing, we also divide the matrix into 5×5 time-frequency areas, which can achieve 96.7% accuracy. The result shows that dividing matrix according to 5-band dividing, instead of average dividing, can improve the classification performance.

E. Source Localization Ablation Experiment

Source localization is the method of converting EEG signals recorded by electrodes to different brain regions introduced

TABLE VI
CLASSIFICATION PERFORMANCE OF FC USING DIFFERENT METHODS

	Accuracy	Precision	Recall	F1 Score
average dividing	95.8%	95.7%	95.8%	95.7%
5-band dividing	96.7%	96.7%	96.5%	96.6%

in Section IV-B, which can better eliminate volumetric conduction effect of EEG. Fig. 9(c) shows the change of precision-recall curve with and without source localization, which shows that source localization can improve classification performance. We can further analyze the impact of cerebrovascular cognitive impairment on EEG activity in specific brain regions by source localization.

VI. CONCLUSION

This work has developed Cog-EEG, an approach to distinguish healthy people, cerebrovascular patients with cognitive impairment and cerebrovascular patients without cognitive impairment using low-density EEG signals. The main contribution of this article is that we collect a dataset of healthy people, cerebrovascular patients with and without cognitive impairment, exploit wMNE to enable source localization with low-density EEG signals, apply XWT to EEG signal correlation, and establish function connection matrix. 96.7% classification accuracy is achieved on low-density EEG signals. By comparing our work with existing work (Adebisi et al. [5]), it demonstrates XWT can increase the accuracy. Also, we conducted source localization ablation experiment, which demonstrates source localization can improve classification performance. Future works would focus on expanding the dataset for large-scale validation.

REFERENCES

- [1] L. Torres-Simón, S. Doval, A. Nebreda, S. J. Llinas, E. B. Marsh, and F. Maestú, "Understanding brain function in vascular cognitive impairment and dementia with EEG and MEG: A systematic review," *NeuroImage. Clin.*, vol. 35, Jan. 2022, Art. no. 103040.
- [2] L. Chu, L. Pei, and R. Qiu, "Ahed: A heterogeneous-domain deep learning model for IoT-enabled smart health with few-labeled EEG data," *IEEE Internet Things J.*, vol. 8, no. 23, pp. 16787–16800, Dec. 2021.
- [3] S. Lu, Y. Xia, W. Cai, M. Fulham, and D. D. Feng, "Early identification of mild cognitive impairment using incomplete random forest-robust support vector machine and FDG-PET imaging," *Comput. Med. Imag. Graph.*, vol. 60, pp. 35–41, Sep. 2017.

- [4] S. Das and S. D. Puthankattil, "Complex network analysis of MCI-AD EEG signals under cognitive and resting state," *Brain Res.*, vol. 1735, May 2020, Art. no. 146743.
- [5] A. T. Adebisi, V. Gonuguntla, H.-W. Lee, and K. C. Veluvolu, "Classification of dementia associated disorders using EEG based frequent subgraph technique," in *Proc. IEEE Int. Conf. Data Min. Workshops (ICDMW)*, 2020, pp. 613–620.
- [6] W. Xie, R. T. Toll, and C. A. Nelson, "EEG functional connectivity analysis in the source space," *Develop. Cogn. Neurosci.*, vol. 56, Aug. 2022, Art. no. 101119.
- [7] M. Murugappan, M. Rizon, R. Nagarajan, S. Yaacob, D. Hazry, and I. Zunaidi, "Time-frequency analysis of EEG signals for human emotion detection," in *Proc. 4th Kuala Lumpur Int. Conf. Biomed. Eng.*, 2008, pp. 262–265.
- [8] P. Arias-Cabarcos, T. Habrich, K. Becker, C. Becker, and T. Strufe, "Inexpensive brainwave authentication: New techniques and insights on user acceptance," in *Proc. 30th USENIX Secur. Symp. (USENIX Security)*, 2021, pp. 55–72.
- [9] C. Ieracitano, N. Mammone, A. Bramanti, A. Hussain, and F. C. Morabito, "A convolutional neural network approach for classification of dementia stages based on 2D-spectral representation of EEG recordings," *Neurocomputing*, vol. 323, pp. 96–107, Jan. 2019.
- [10] A. B. Rabeh, F. Benzarti, and H. Amiri, "Diagnosis of Alzheimer diseases in early step using SVM (support vector machine)," in *Proc. 13th Int. Conf. Comput. Graph., Imag. Vis. (CGIV)*, 2016, pp. 364–367.
- [11] P. Chen et al., "Four distinct subtypes of Alzheimer's disease based on resting-state connectivity biomarkers," *Biol. Psy.*, vol. 93, no. 9, pp. 759–769, 2022.
- [12] Y. Ding et al., "Fully automated discrimination of Alzheimer's disease using resting-state electroencephalography signals," *Quant. Imag. Med. Surg.*, vol. 12, no. 2, pp. 1063–1078, 2022.
- [13] M. Bayot et al., "Functional networks underlying freezing of gait: A resting-state electroencephalographic study," *Neurophysiologie Clinique*, vol. 52, no. 3, pp. 212–222, 2022.
- [14] Q. Zhang, P. Wang, S. Li, and Y. Jing, "A portable real-time EEG signal acquisition and tele-medicine system," *J. Comput. Methods Sci. Eng.*, vol. 21, no. 4, pp. 891–901, 2021.
- [15] Y. Huang et al., "How different EEG references influence sensor level functional connectivity graphs," *Front. Neurosci.*, vol. 11, p. 368, Jul. 2017.
- [16] J. Lu, R. Cai, Z. Guo, Q. Yang, K. Xie, and S. Xie, "Dual-stream attention-TCN for EMG removal from a single-channel EEG," *IEEE Internet Things J.*, vol. 11, no. 11, pp. 19575–19588, Jun. 2024.
- [17] G. Sahonero and H. Calderon, "A comparison of SOBI, FastICA, JADE and infomax algorithms," in *Proc. 8th Int. Multi-Conf. Complex., Informat. Cybernet.*, 2017, pp. 17–22.
- [18] Z. Zhang, Y. Liu, and S.-h. Zhong, "GANSER: A self-supervised data augmentation framework for EEG-based emotion recognition," *IEEE Trans. Affect. Comput.*, vol. 14, no. 3, pp. 2048–2063, Jul./Sep. 2023.
- [19] Y. Zhang et al., "Identification of psychiatric disorder subtypes from functional connectivity patterns in resting-state electroencephalography," *Nature Biomed. Eng.*, vol. 5, no. 4, pp. 309–323, 2021.
- [20] M. Huang et al., "MEG source imaging method using fast L1 minimum-norm and its applications to signals with brain noise and human resting-state source amplitude images," *NeuroImage*, vol. 84, pp. 585–604, Jan. 2014.
- [21] Y. Li et al., "Biased orientation and color tuning of the human visual gamma rhythm," *J. Neurosci.*, vol. 42, no. 6, pp. 1054–1067, 2022.
- [22] R. Ashenaei, A. A. Beheshti, and T. Y. Rezaii, "Stable EEG-Based biometric system using functional connectivity based on time-frequency features with optimal channels," *Biomed. Signal Process. Control*, vol. 77, Aug. 2022, Art. no. 103790.
- [23] C. Wang et al., "MI-EEG classification using Shannon complex wavelet and convolutional neural networks," *Appl. Soft Comput.*, vol. 130, Nov. 2022, Art. no. 109685.
- [24] P. P. Vijayakumaran, D. Narzary, V. Gonuguntla, H.-W. Lee, and K. C. Veluvolu, "EEG based functional connectivity analysis of Alzheimer's disease subjects," in *Proc. Int. Conf. Artif. Intell. Inf. Commun. (ICAIIIC)*, 2020, pp. 356–361.
- [25] M. Hassan and F. Wendling, "Electroencephalography source connectivity: Aiming for high resolution of brain networks in time and space," *IEEE Signal Process. Mag.*, vol. 35, no. 3, pp. 81–96, May 2018.
- [26] S. Mao, A. Mordret, M. Campillo, H. Fang, and R. D. van der Hilst, "On the measurement of seismic traveltimes changes in the time-frequency domain with wavelet cross-spectrum analysis," *Geophys. J. Int.*, vol. 221, no. 1, pp. 550–568, 2019.



Xiaomin Guo received the M.S. degree in surgery from Xi'an Jiaotong University, Xi'an, China, in 2009, where she is currently pursuing the Ph.D. degree in neurology.

She is currently an Associate Professor (Deputy Chief Neurologist) with the Department of Neurology, Shaanxi Provincial Hospital, Xi'an, where she also serves as the Deputy Director. She is the Project Investigator of the Key Industrial Innovation Chain Project in Shaanxi. She has over 15 years experiences on the diagnosis and treatment small vessel diseases, and cognitive dysfunction. Her research interests include applications of electroencephalogram signal processing technology in neurological diseases.



Luting Shen received the undergraduate degree from the College of Information Technology, Shanghai Jian Qiao University, Shanghai, China, in 2023. She is currently pursuing the M.S. degree with the School of Computer Science and Technology, Donghua University, Shanghai. Her research interests include security and privacy in mobile networks.



Lan Li received the bachelor's degree in software engineering from Anhui University, Hefei, China, in 2021, and the M.S. degree in software engineering from Donghua University, Shanghai, China, in 2024.

She is currently a Teacher with Anhui Sanlian University, Hefei. Her research interests include electroencephalography and image segmentation.



Shan Chang (Member, IEEE) received the Ph.D. degree in computer software and theory from Xi'an Jiaotong University, Xi'an, China, in 2012.

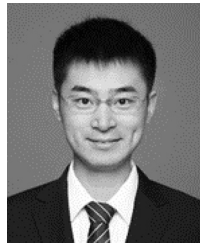
From 2009 to 2010, she was a Visiting Scholar with the Department of Computer Science and Engineering, Hong Kong University of Science and Technology, Hong Kong. She was also a Visiting Scholar with the BBCR Lab, University of Waterloo, Waterloo, ON, Canada, from 2010 to 2011. She is currently a Professor with the Department of Computer Science and Technology, Donghua University, Shanghai, China. Her research interests include security and privacy in Internet of Things, participatory sensing, and federated learning.

Prof. Chang is a member of the IEEE Computer Society, Communication Society, and Vehicular Technology Society.



Zongwei Liu received the B.S. degree in information technology and the Ph.D. degree in underwater acoustics engineering from Northwestern Polytechnical University, Xi'an, China, in 2008 and 2013, respectively.

From 2013 to 2021, he was a Research Assistant with the First Institute of Oceanography, Ministry of Natural Resources, Qingdao, China, where he has been a Senior Engineer since 2021. His research interests include robust acoustic signal processing, ocean noise analysis, and ocean acoustic prediction based on the ocean model.



Yang Shi (Member, IEEE) received the B.S. and M.S. degrees in electronic engineering and the Ph.D. degree in underwater acoustics engineering from Northwestern Polytechnical University, Xi'an, China, in 2009, 2012, and 2017, respectively.

From September 2017 to September 2020, he worked as a Postdoctoral Fellow with the College of Oceanic and Atmospheric Science, Ocean University of China, Qingdao, China. Since September 2020, he has been working as a Full Professor with the School of Marine Science and Technology, Northwestern Polytechnical University. His research interests include signal processing.